Physics Letters A 374 (2010) 1063–1067

Contents lists available at ScienceDirect

Physics Letters A

www.elsevier.com/locate/pla

Macroscopic far-field observation of the sub-wavelength near-field dipole vortex

Xin Li, Henk F. Arnoldus *

Department of Physics and Astronomy, Mississippi State University, PO Drawer 5167, Mississippi State, MS 39762-5167, United States

ARTICLE INFO

Article history:
Received 30 November 2009
Accepted 9 December 2009
Available online 21 December 2009
Communicated by V.M. Agranovich

Keywords:
Optical vortex
Dipole radiation
Near field
Far field

ABSTRACT

The energy flow lines of the radiation emitted by a rotating electric dipole moment have a vortex structure near the source. The spatial extend of this vortex is well below an optical wavelength. This near-field vortex has a macroscopic effect which could be observed in the far field.

1. Introduction

When a small object (atom, molecule, nano-particle) is placed in an external electromagnetic field (laser beam), oscillating with angular frequency ω, a current density will be induced in the particle which also oscillates harmonically with angular frequency ω. In a multipole expansion of the current density [1] the leading term is the electric dipole moment, and we shall assume that this contribution dominates the remaining terms. The induced dipole moment can be written as

$$\mathbf{d}(t) = d_0 \,\mathrm{Re}\big(\boldsymbol{\varepsilon} e^{-i\omega t}\big), \tag{1}$$

with d_0 a constant (real) and $\boldsymbol{\varepsilon}$ a complex-valued unit vector, normalized as $\boldsymbol{\varepsilon}\cdot\boldsymbol{\varepsilon}^* = 1$. The oscillating dipole moment emits electromagnetic radiation. The emitted electric field has the form

$$\mathbf{E}(\mathbf{r},t) = \mathrm{Re}\big[\mathbf{E}(\mathbf{r})e^{-i\omega t}\big], \tag{2}$$

with $\mathbf{E}(\mathbf{r})$ the complex amplitude, and the magnetic field $\mathbf{B}(\mathbf{r},t)$ can be represented similarly. The flow of energy in the radiation field is determined by the Poynting vector $\mathbf{S}(\mathbf{r},t)$: the direction of the vector $\mathbf{S}(\mathbf{r},t)$ at the field point $\mathbf{r}$ is the direction of energy flow, and the magnitude of $\mathbf{S}(\mathbf{r},t)$ at this point is the power transport through a unit area into the direction of $\mathbf{S}(\mathbf{r},t)$. For a time-harmonic field, the Poynting vector can be expressed in terms of the complex amplitudes of the electric and magnetic fields as

$$\mathbf{S}(\mathbf{r}) = \frac{1}{2\mu_0}\,\mathrm{Re}\big[\mathbf{E}(\mathbf{r})\times\mathbf{B}(\mathbf{r})^*\big]. \tag{3}$$

Here, terms that oscillate at twice the optical frequency have been dropped, since they average to zero on a time scale of an optical cycle, and this makes the Poynting vector independent of time. The Poynting vector $\mathbf{S}(\mathbf{r})$ defines a vector field in space, and its field lines are the trajectories of energy flow.

In the geometrical optics limit of light propagation [2], where variations in the optical field on a sub-wavelength scale are neglected, the field lines of the Poynting vector of the radiation emitted by any localized source are straight lines. These optical rays run radially outward from the (point) source to the far field. Furthermore, at a large distance from any localized source, as compared to the wavelength, the field lines of the Poynting vector asymptotically approach straight lines. Therefore, any curving in the energy flow lines can only occur close to a source (the near field) and the flow pattern must have a sub-wavelength structure. In this Letter we shall show that such a nanoscopic energy flow pattern in the near field can have an observable, macroscopic effect in the far field.

2. The Poynting vector

The complex amplitudes $\mathbf{E}(\mathbf{r})$ and $\mathbf{B}(\mathbf{r})$ for the radiation emitted by an electric dipole are well known [3], and the Poynting vector can easily be constructed. The result for a dipole located at the origin of coordinates is [4]

$$\mathbf{S}(\mathbf{r}) = \frac{3P_0}{8\pi r^2}\left\{\big[1-(\hat{\mathbf{r}}\cdot\boldsymbol{\varepsilon})(\hat{\mathbf{r}}\cdot\boldsymbol{\varepsilon}^*)\big]\hat{\mathbf{r}} - \frac{2}{q}\left(1+\frac{1}{q^2}\right)\mathrm{Im}\big[(\hat{\mathbf{r}}\cdot\boldsymbol{\varepsilon})\boldsymbol{\varepsilon}^*\big]\right\}, \tag{4}$$

* Corresponding author.
E-mail addresses: xl121@msstate.edu (X. Li), hfa1@msstate.edu (H.F. Arnoldus).

0375-9601/$ – see front matter
doi:10.1016/j.physleta.2009.12.034

where P_0 is the total emitted power and $\hat{\mathbf{r}}$ is the radial unit vector into the observation direction. We shall use dimensionless coordinates with the wave number $k_0 = \omega/c$ as scale factor. In this way, a dimensionless distance of 2π corresponds to one optical wavelength. In Eq. (4) we have set $q = k_0 r$ for the dimensionless distance between the dipole and the field point.

When an atom or other small particle is irradiated by a linearly polarized laser beam, vector $\boldsymbol{\varepsilon}$ is real, and along the polarization direction of the incident field. Then the dipole moment is $\mathbf{d}(t) = d_0\boldsymbol{\varepsilon}\cos(\omega t)$, and it oscillates linearly along the $\boldsymbol{\varepsilon}$ direction. The term $\mathrm{Im}[(\hat{\mathbf{r}}\cdot\boldsymbol{\varepsilon})\boldsymbol{\varepsilon}^*]$ in the Poynting vector vanishes and $\mathbf{S}(\mathbf{r})$ is proportional to $\hat{\mathbf{r}}$. Therefore, the field lines run radially outward from the location of the dipole, and they are straight at all distances. For a circularly polarized laser, the dipole moment $\mathbf{d}(t)$ rotates along a circle. In the most general state of oscillation, the dipole moment $\mathbf{d}(t)$ traces out an ellipse in a plane [5,6]. We take this plane as the xy-plane, and let the axes of the ellipse coincide with the coordinate axes. A convenient parametrization of vector $\boldsymbol{\varepsilon}$ is then

$$\boldsymbol{\varepsilon} = -\frac{1}{\sqrt{\beta^2+1}}(\beta\mathbf{e}_x + i\mathbf{e}_y), \tag{5}$$

with β real, and this gives for the dipole moment

$$\mathbf{d}(t) = -\frac{d_0}{\sqrt{\beta^2+1}}\big[\beta\mathbf{e}_x\cos(\omega t) + \mathbf{e}_y\sin(\omega t)\big]. \tag{6}$$

Vector $\mathbf{d}(t)$ rotates counterclockwise in the xy-plane for $\beta > 0$, and when the sign of β is reversed it rotates clockwise along the same ellipse. For $\beta = \pm 1$ the ellipse reduces to a circle, and for $\beta = 0$ and $\beta \to \pm\infty$ the oscillation becomes linear along the y- and x-axis, respectively.

With $\boldsymbol{\varepsilon}$ given by Eq. (5), the Poynting vector becomes

$$\mathbf{S}(\mathbf{r}) = \frac{3P_0}{8\pi r^2}\left\{1 - \frac{1}{2}\sin^2\theta\left[1 + \frac{\beta^2-1}{\beta^2+1}\cos(2\phi)\right]\right\}\hat{\mathbf{r}} + \frac{3P_0}{8\pi r^2}\frac{2}{q}\left(1+\frac{1}{q^2}\right)\frac{\beta}{\beta^2+1}\sin\theta\,\mathbf{e}_\phi, \tag{7}$$

with (θ,ϕ) the angles in a spherical coordinate system, and $\mathbf{e}_\phi$ the unit vector into the direction of increasing ϕ. The first term on the right-hand side of Eq. (7) is proportional to $\hat{\mathbf{r}}$, so this represents the power outflow in the radially outward direction. The second term is proportional to $\mathbf{e}_\phi$, and this leads to a rotation of the field lines around the z-axis. A typical field line is shown in Fig. 1. The field line swirls around the z-axis numerous times, and then leaves the near field along a smooth curve which asymptotically approaches the straight line ℓ in the figure. It can be shown [7] that all field lines for a rotating dipole (for any β) have a similar appearance as the field line in Fig. 1. Any field line lies on a cone, and a set of field lines forms a vortex structure. For the field line in Fig. 1 we have $\beta = 1$. For larger and smaller values of β the vortex pattern shrinks, until it reaches a point for $\beta = 0$ or $\beta \to \pm\infty$. The vortex in Fig. 1 is of sub-wavelength dimension, since a dimensionless distance of 2π corresponds to one optical wavelength, and for other values of β the spatial extend of the vortex is even smaller.

3. The image of a dipole

When viewed from the far field, the field line of Fig. 1 appears to come from a point in the xy-plane which is displaced with respect to the position of the dipole. Other field lines have a similar rotation, and when an image is formed in the far field it will appear as if the location of the dipole is shifted with respect to the radial direction, indicated by $\hat{\mathbf{r}}_0$ in Fig. 1. In order to determine the

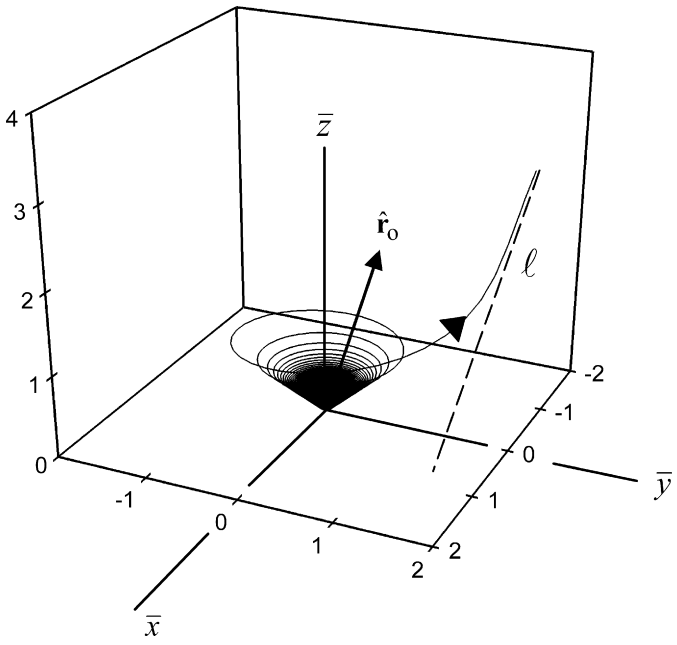

Fig. 1. The figure shows a field line of the Poynting vector for $\beta = 1$. Near the dipole the field line has the appearance of an optical vortex, and in the far field the field line approaches the straight line ℓ. The coordinates are dimensionless, with $\bar{x} = k_0 x$, etc.

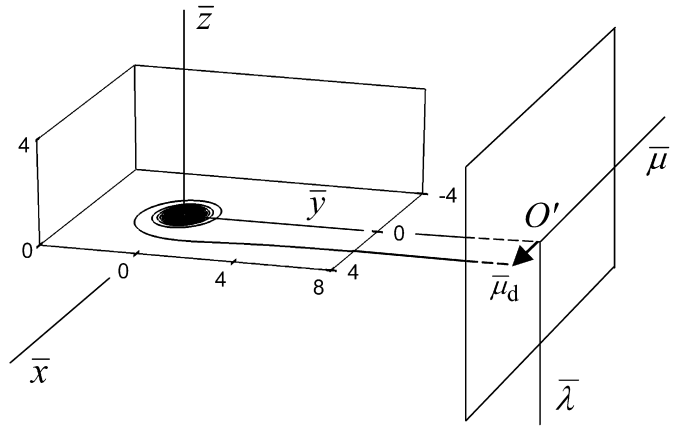

Fig. 2. The figure shows a field line in the xy-plane of the Poynting vector for $\beta = 1$. The field line approaches asymptotically a line parallel to the y-axis, and the image plane is taken to be perpendicular to this field line.

image in the far field we consider a plane, perpendicular to vector $\hat{\mathbf{r}}_0$ in Fig. 1, and at a distance r_0 from the origin. The origin O' of the image plane is represented by vector $\mathbf{r}_0$, and the angles (θ_0,ϕ_0) represent the direction of $\hat{\mathbf{r}}_0$, which is the direction of observation. In this image plane we set up a Cartesian coordinate system (λ,μ), such that the coordinate axes are directed along the corresponding unit vectors $\mathbf{e}_{\theta_0}$ and $\mathbf{e}_{\phi_0}$, respectively, in the spherical coordinate system. Fig. 2 illustrates the setup for the case of $\theta_0 = \phi_0 = \pi/2$, for which the observation plane is perpendicular to the y-axis. We use dimensionless coordinates $\bar{\lambda} = k_0\lambda$, $\bar{\mu} = k_0\mu$ for points in the plane.

The experimentally observed quantity is the intensity on the image plane, which is defined as

$$I(\lambda,\mu;\beta) = \mathbf{S}(\mathbf{r})\cdot\hat{\mathbf{r}}_0. \tag{8}$$

Here, $\mathbf{S}(\mathbf{r})$ is the Poynting vector at point $\mathbf{r}$ in the image plane, and $\hat{\mathbf{r}}_0$ is the unit normal on the image plane. The intensity depends on the coordinates (λ,μ) in the image plane, the parameter β of the

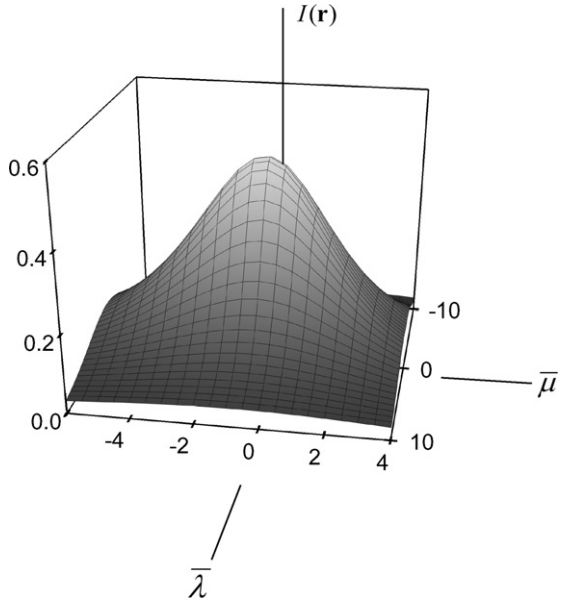

Fig. 3. The figure shows the intensity distribution over an image plane, located at $\theta_0 = \phi_0 = \pi/2$, for a circular dipole with $\beta = 1$. The maximum is located at $\bar{\lambda} = 0$, $\bar{\mu} = -2/3$, and its shift with respect to the origin of the image plane is due to the vortex in the near field.

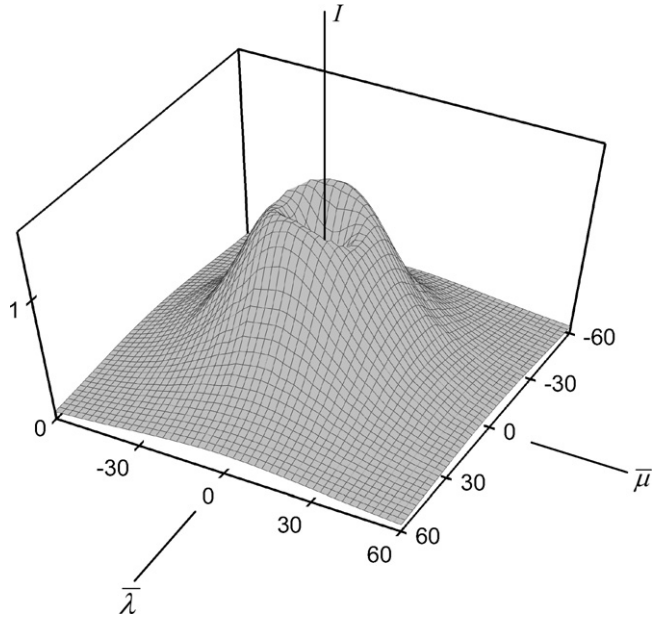

Fig. 4. The figure shows the intensity distribution for an elliptical dipole moment with $\beta = 0.4$, and for observation in the same image plane as in Fig. 3. The minimum of the hole is located at $\bar{\lambda} = 0$, $\bar{\mu} = 2/3$, but that cannot be seen in the figure.

ellipse, and the coordinates (r_0, θ_0, ϕ_0) of the origin of the image plane. The intensity can be evaluated explicitly, and the result is

$$I(\lambda, \mu; \beta) = I_0 \left(\frac{q_0}{q}\right)^3 \left\{1 - \frac{1}{q^2}\frac{1}{1+\beta^2}\left[\beta^2(\bar{\rho}\cos\phi_0 - \bar{\mu}\sin\phi_0)^2 + (\bar{\rho}\sin\phi_0 + \bar{\mu}\cos\phi_0)^2\right] - \frac{1}{q_0 q}\left(1 + \frac{1}{q^2}\right)\frac{2\beta}{\beta^2+1}\bar{\mu}\sin\theta_0\right\}, \tag{9}$$

with $q_0 = k_0 r_0$ and $I_0 = 3P_0/(8\pi r_0^2)$. Here we have introduced the abbreviation

$$\bar{\rho} = q_0 \sin\theta_0 + \bar{\lambda}\cos\theta_0. \tag{10}$$

Fig. 3 shows the intensity distribution over the image plane for the same parameters as in Fig. 2. The central field line in Fig. 2 is displaced along the $\bar{\mu}$-axis and it crosses the axis at $\bar{\mu}_d = -2$. The intensity profile of Fig. 3 has a peak at $\bar{\mu} = -2/3$ on the $\bar{\mu}$-axis, which is a result of the shift of the field lines, which in turn is a result of the rotation of the field lines near the dipole. It can be shown [8] that the location of the peak is independent of the distance q_0 between the dipole and the observation plane, so this shift is amenable to observation in the far field.

The intensity profile in Fig. 3 is for observation perpendicular to the y-axis, as in Fig. 2, and for the case of a circular dipole with$\beta = 1$. Fig. 4 shows the intensity distribution over the same plane, but now for an elliptical dipole with $\beta = 0.4$. It appears that the peak has turned into a hole, and it can be shown that this hole is located at $\bar{\mu} = +2/3$. Therefore, the rotation of the field lines can result in a shifted peak or a shifted hole in the far field, depending on the eccentricity of the ellipse. For other observation directions (θ_0, ϕ_0) a variety of other intensity distributions are possible.

4. The difference profile

The shifts of the peak in Fig. 3 and the hole in Fig. 4 are of the same order of magnitude as the spatial extend of the dipole vortex in Fig. 1. On one hand, this shift leads to a possible observation of the dipole vortex through a measurement in the far field, but on the other hand, this shift is extremely small. It also requires a precise calibration of the experimental setup, since the shift is measured with respect to the origin O' of the image plane. Furthermore, the profile has a large background, as can be seen from the figures, and the shape of this background (peak, hole or a more complicated distribution) depends on the observation angles θ_0, ϕ_0, and on the parameter β of the ellipse.

The shift of the peak or hole depends on the sign of β. The peak in Fig. 3 moves to $\bar{\mu} = +2/3$ when we reverse the direction of rotation of the dipole, so when we change the sign of β. This is obvious from Fig. 2, since changing the direction of rotation results in the field lines swirling around the z-axis in the opposite direction. The asymmetry in the intensity distribution comes from the rotation of the field lines near the source. In an experiment, changing the direction of rotation can be accomplished by changing the helicity of the driving laser, and this would result in the moving of the peak or hole to the opposite direction. We now introduce the difference profile

$$\Delta I(\lambda, \mu; \beta) = I(\lambda, \mu; \beta) - I(\lambda, \mu; -\beta). \tag{11}$$

The idea is that in this difference the large background will cancel, and only the asymmetry due to the rotation of the field lines will contribute to this profile. Therefore, any observation of $\Delta I \neq 0$ in the far field would confirm the rotation of the field lines in the near field.

From Eq. (9) we find

$$\Delta I(\lambda, \mu; \beta) = -\frac{\varsigma}{q^4}\left(1 + \frac{1}{q^2}\right)\bar{\mu}, \tag{12}$$

with

$$\varsigma = \frac{3P_0 k_0^2}{2\pi}\frac{\beta}{\beta^2+1}\sin\theta_0, \tag{13}$$

and

$$q = \sqrt{q_0^2 + \bar{\lambda}^2 + \bar{\mu}^2}, \tag{14}$$

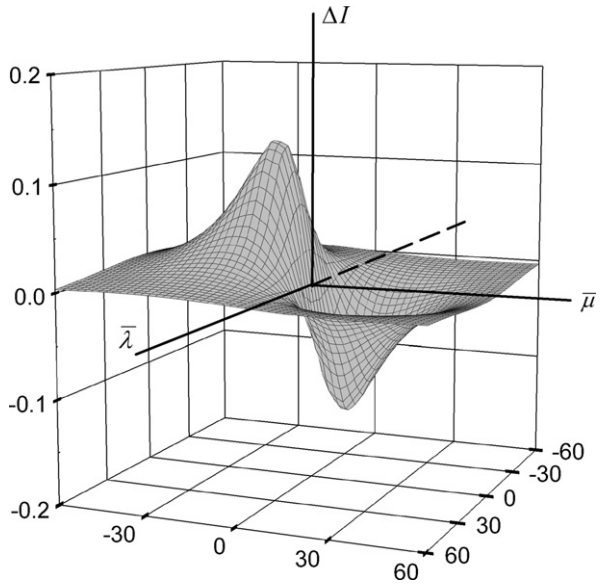

Fig. 5. The difference profile ΔI in the $(\bar{\lambda},\bar{\mu})$ plane is shown for $q_0 = 20$ and β positive. The maxima and minima are located on the $\bar{\mu}$-axis at $\bar{\mu} = -11.5$ and $\bar{\mu} = 11.5$, respectively.

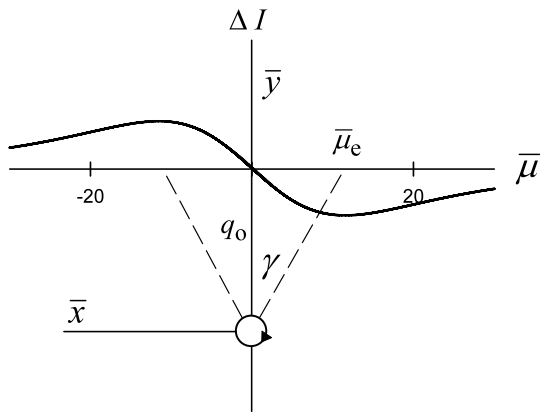

Fig. 6. The extrema on the $\bar{\mu}$-axis are located at $\bar{\mu}_e$ and $-\bar{\mu}_e$. For $\beta > 0$, as in the figure, the maximum is at the negative side of the $\bar{\mu}$-axis. Both extrema appear under angle γ as seen from the location of the dipole. For the figure we took $q_0 = 20$, which is just over three optical wavelengths. Here, $\gamma = 30°$, and when we increase q_0 this angle remains 30°.

as the dimensionless distance between the dipole and the observation point in the image plane. The difference profile is independent of the observation angle ϕ_0, and the dependence on θ_0 only enters through $\sin\theta_0$ in the overall factor ς. Therefore, $\Delta I = 0$ for observation on the z-axis. The parameter β of the ellipse only appears in the overall constant ς. Consequently, apart from an overall constant, the difference profile is independent of the observation angles and is the same for any ellipse.

The profile in the image plane is a function of the dimensionless coordinates $\bar{\lambda}$ and $\bar{\mu}$, with q_0 as the only parameter. The function ΔI is symmetric in $\bar{\lambda}$ and antisymmetric in $\bar{\mu}$. It is easily verified from Eqs. (12) and (14) that ΔI has two extrema on the $\bar{\mu}$-axis, symmetrically located with respect to the origin. Fig. 5 shows ΔI for $q_0 = 20$, and β positive. For β negative, the overall constant ς changes sign and the maximum and minimum switch positions. If we indicate the positions of the extrema by $\pm\bar{\mu}_e$, then for the far field, where $q_0 \gg 1$, we obtain

$$\bar{\mu}_e = \frac{q_0}{\sqrt{3}}. \tag{15}$$

The location of the peak in Fig. 3 is at $\bar{\mu} = -2/3$, and this is a displacement of about one-tenth of a wavelength with respect to the origin. The extrema of the difference profile are proportional to q_0, so their location is proportional to the distance between the dipole and the image plane. Therefore, these extrema are at macroscopic distances from the origin, even though they are a result of the microscopic vortex near the dipole. Fig. 6 shows the location of the extrema with respect to the dipole. As viewed from the dipole, they appear under an angle γ, with $\tan\gamma = \bar{\mu}_e/q_0$, and this gives $\gamma = 30°$.

The expression for the difference profile holds for all distances q_0. If ΔI would be measured in the near field, for which $q_0 \ll 1$, we would have $\bar{\mu}_e/q_0 = 1/\sqrt{5}$, and this would give $\gamma = 24°$. Therefore, the angular positions of the extrema are in the range $24° < \gamma < 30°$.

In a recent experiment [9] the difference profile was measured for a small polystyrene sphere with a diameter of 4.6 μm in a circularly polarized laser beam with a wavelength of 532 nm. The observation angle was $\theta_0 = \pi/2$. The experimental results are in good qualitative agreement with Fig. 6. In the experimental data there are some small oscillations in the wings which are probably due to the finite size of the object.

5. Conclusions

Radiation emitted by a rotating electric dipole moment exhibits a vortex pattern in the energy flow lines. This vortex is present in the near field of the source, and is of sub-wavelength dimension. In the far field, the field lines approach asymptotically straight lines, but these field lines are slightly displaced with respect to the radially outward direction. This gives the perception that the location of the dipole is displaced with respect to its actual position. When the intensity is measured on an observation plane, perpendicular to the radial direction, the image of the dipole is slightly shifted with respect to the origin, and this is a result of the rotation of the field lines in the near field. In this fashion, the vortex in the near field could be observed as a shift of the image in the far field. This shift, however, is of sub-wavelength order, which may be difficult to detect.

We propose to detect the vortex in the near field through a measurement of the difference profile in the far field. The intensity for a rotating dipole is measured at a given point in the observation plane. Then the helicity of the driving laser is reversed, and the new intensity is subtracted from the first. We have shown that this difference profile is a universal function, with only the distance between the dipole and the observation plane as a free parameter. Apart from an overall factor for a given observation plane and state of rotation of the dipole (the β of the ellipse), any profile has a peak and a hole as shown in Fig. 5. The location of the extrema is independent of the angular position (θ_0,ϕ_0) of the observation plane, and independent of the magnitude of β. When β changes sign, the peak and the hole reverse positions. The most important property of the difference profile is that the locations of the extrema are not of sub-wavelength order. The angular location γ of the extrema, as shown in Fig. 6, is 30° when the profile is observed in the far field (a few wavelengths or more from the dipole). The distance between the peak and the hole is proportional to the distance between the dipole and the observation plane, since γ remains constant. Therefore, the separation between the extrema is of macroscopic order, even though they are a result of the nanoscopic vortex near the source. Without the vortex, the difference profile would be identically zero, and consequently any macroscopic far-field observation of a ΔI as in Fig. 5 would confirm the existence of this vortex.

References

[1] J. van Bladel, Singular Electromagnetic Fields and Sources, Clarendon Press, Oxford, 1991, Section 2.9.
[2] M. Born, E. Wolf, Principles of Optics, 6th edition, Pergamon, Oxford, 1980, Chapter 3.
[3] J.D. Jackson, Classical Electrodynamics, 3rd. ed., Wiley, New York, 1999, p. 411.
[4] H.F. Arnoldus, J.T. Foley, Opt. Commun. 231 (2004) 115.
[5] I.V. Lindell, Methods for Electromagnetic Field Analysis, Oxford University Press, Oxford, 1992, Section 1.4.
[6] L. Mandel, E. Wolf, Optical Coherence and Quantum Optics, Cambridge University Press, Cambridge, 1995, p. 469.
[7] J. Shu, X. Li, H.F. Arnoldus, J. Mod. Opt. 55 (2008) 2457.
[8] J. Shu, X. Li, H.F. Arnoldus, J. Opt. Soc. Am. A 26 (2009) 395.
[9] D. Haefner, S. Sukhov, A. Dogariu, Phys. Rev. Lett. 102 (2009) 123903.